RESEARCH PAPER

Corrosion Inhibition Performance of a Schiff Base on Copper in HNO_3 and H_2SO_4 Solutions: Electrochemical and Adsorption Investigations

C. Nirmala[1], S. Annapoorani[2], E. Dhanasekaran[3], K. Velumani[4], P. Palani Murugan[4], S.Rameshkumar[4*]

[1]*Department of Chemistry, Akshaya College of Engineering and Technology, Kinathukadavu, Tamilnadu – 642109.*
[2]*Department of Chemistry, LRG government Arts College for women, Tiruppur, Tamilnadu-641604.*
[3]*Department of Chemistry, Nandha College of Technology,Erode, Tamilnadu- 638052.*
[4]*Department of Chemistry, Sri Vasavi College, Erode, Tamilnadu-638316.*

Received: ; Revised: ; Accepted: ; Available Online:

ABSTRACT
The ability of 1, 3-bis (pyridin-2-ylmethylene) urea to inhibit copper corrosion in 1.0 M HNO_3 and 0.5 M H_2SO_4 was studied using weight measurements and electrochemical measurements. The inhibition efficiency is notable as the Schiff base shows nearly 95% inhibition at 1.0 mM. The electrochemical studies showed increased charge transfer resistance and decreased corrosion current density due to the formation of a protective adsorbed film on the copper surface. Polarization measurements showed a mixed type inhibition but predominantly cathodic. The adsorption data describes the Langmuir isotherm, and thermodynamic parameters reveal that the adsorption process is spontaneous and physico–chemical in nature. The effectiveness of the inhibitor is mainly associated with the nitrogen donor atoms and the conjugated π-electron system which promotes a stable surface coverage.

Keywords: *Schiff base; Electrochemical Impedance Spectroscopy (EIS); Corrosion Inhibition;Adsorption Isotherm;Potential of zero charge (PZC).*

How to cite this article: Nirmala C, Annapoorani S, Dhanasekaran E, Velumani K, Murugan PP, Rameshkumar S. Corrosion Inhibition Performance of a Schiff Base on Copper in HNO_3 and H_2SO_4 Solutions: Electrochemical and Adsorption Investigations. Int J Drug Deliv Technol. 2026;16(54s): 381-393. DOI: 10.25258/ijddt.16.54s.33
Source of support: Nil.
Conflict of interest: None

Introduction

Copper corrosion in acidic media is an electrochemical process that can greatly hamper the performance and durability of metals [1]. Copper generally tends to undergo pitting during use, although they usually do not penetrate quite through the copper. Corrosion in sulfuric acid involves anodic dissolution, and formation of sulfate complexes with copper ions. Nitric acid can play a role in either passivation or localized pitting, depending on the concentration, due to the dual acid-oxidant character [4]. Ensuring effective control of copper corrosion in such environments is paramount to maintaining the integrity of electrical systems, plumbing components, and processing equipment.

Organic corrosion inhibitors have a large area of application as they are effective at relatively low concentrations and can generate protective surface films. One of them Schiff Base Compounds containing azomethine (–C=N–) functional group has gained considerable attention as a new corrosion inhibitor [6]. The inhibition performance of these compounds is mainly related to the presence of heteroatoms (N, O, S) and π-electron systems which can adsorb on metal surfaces [7]. This adsorption slows corrosion by blocking the active sites on the metal surface and reducing metal dissolution and cathodic reactions [8]. Moreover, Schiff bases can produce complexes with Cu^+ and Cu^{2+} ions further stabilizing the protective layer too [9]. The strength of adsorption and efficiency of inhibitors are considerably affected by structural factors such as planarity, aromatic character, and electronic effects of substituents [10].

In general, Schiff bases are synthesized via condensation reactions between primary amines and aldehydes or ketones [11]. The molecular structure can be changed to improve properties such as solubility and surface interaction with copper [12]. The effectiveness of these inhibitors is often evaluated by weight-loss measurements, Potentiodynamic polarization and electrochemical impedance spectroscopy (EIS). Often it is not possible to distinguish between physical or chemical adsorption mechanisms just by the thermodynamic parameters like ΔG°ads and ΔH°ads [13]. Numerous Schiff base inhibitors demonstrate mixed-type inhibition, reducing both anodic and cathodic corrosion processes [14].

In sulfuric acid media (H_2SO_4), adsorption could be poorly affected due to competition between inhibitor molecules and sulfate ions for active sites on the surface. However, suitably designed Schiff bases can effectively bypass this limitation [15]. In nitric acid, oxidizing nature of the

*Author for Correspondence:srkresearch22@gmail.com

medium can modify the stability of inhibitor or facilitate passive film formation.

Thus, oxidative resistance is an important parameter for inhibitor design [16]. Maximum efficiency of inhibition is generally obtained at optimum concentration, at which the surface cover is almost complete [17].

Quantum chemical methods are used more and more to relate molecular electronic properties, particularly those developed through density functional theory (DFT), with inhibition behavior [18]. Frontier molecular orbital energies, charge distribution, HOMO–LUMO energy gap, and dipole moment help in understanding adsorption tendency and inhibition performance [19]. Adsorption behavior is usually interpreted using isotherm models such as Langmuir, Temkin and Frumkin. For practical use, it's an essential condition that the ideal inhibitor is environmentally friendly and cost-effective. Recent reports show that some Schiff base compounds inhibit the corrosion of metals to over 80–90% in acidic media [21]. Analyzing the performance of inhibitors requires the application of electrochemical and surface characterization techniques for mechanistic understanding [22].

The stability of inhibitor film under electrochemical conditions in the acidic medium is especially important for copper protection [23]. Spectroscopic methods like UV-Vis, FTIR and XPS can be used to verify metal–inhibitor complex formation. Temperature dependent studies also help to discriminate the chemisorption from exothermic physisorption [24]. Impedance measurements often correlate inhibition with an increase in charge-transfer resistance and a change in double-layer capacitance, whereas polarization investigations suggest mixed-type inhibition.

In the presence of highly oxidizing nitric acid solutions, the inhibitor efficacy may decline unless its molecular structure is stabilized by appropriate substituents [25]. Including chelating groups on the one hand and a thiazole, pyridine or imidazole moiety rich in heteroatom on the other can improve adsorption, increase complex formation and improve film stability [26,27]. Recent trends also highlight the adoption of environmentally friendly synthesis strategies and biodegradable precursors to minimize environmental damage. In certain systems, the presence of halide ions or metal cations can enhance the inhibition efficiency synergy.

To evaluate something reliably, the experiments must necessarily be done under consistent and standardized conditions such as proper specimen preparation, controlled aeration and correct temperature. We can compare the efficacy of the Schiff base to that of established inhibitors such as benzotriazole. Long-term exposure studies are necessary to establish the longevity and self-healing capacity of protective films. Surface analysis indicates that copper surfaces in the presence of inhibitors are smoother and less corroded than uninhibited copper surfaces.

In general, Schiff base compounds can be used to rationally and effectively control copper corrosion in H2SO4 and HNO3 media. The tunability of the molecular structure along with electrochemical testing, surface characterization and computation of the introduced systems provides a valid framework for their evaluation in terms of efficacy. As a result, it seems likely that future work will focus on improving nitric acid oxidative stability, green synthesis, and validating in industry performance. This method has a significant potential for safe, economical, and sustainable corrosion protection for copper in acidic environments.

Experiments

2.1 Materials

For weight-loss experiments, copper specimens of dimensions 2.5 cm × 1 cm × 0.1 cm were employed, with the following composition (wt.%): 0.002 Ni, 0.020 Al, 0.001 Mn, 0.116 Si, with the balance being Cu. Prior to testing, the specimens were mechanically polished using emery papers of successive grades (1/0, 2/0, 3/0, 4/0, and 5/0), degreased with acetone, and dried thoroughly.

For polarization and electrochemical impedance studies, a Teflon-coated cylindrical copper electrode with an exposed surface area of 0.2826 cm^2 and the same composition as described above was used. Before each measurement, the electrode surface was cleaned with acetone, dried under nitrogen, and polished to a mirror finish using emery papers of progressively finer grades (1/0 to 5/0). Surface cleanliness was confirmed when the electrode exhibited complete and uniform wettability with water.

All experiments were conducted at room temperature, maintained at 301 ± 1 K. Test solutions were prepared using double-distilled water, while all chemicals used for preparing stock acid solutions were of analytical reagent grade and obtained from Sigma Aldrich and E. Merck (India).

2.2 Synthesis of Schiff base

A minimum quantity of ethanol was used to dissolve 2-formylpyridine and urea in a 2:1 molar ratio. The two solutions were combined and stirred continuously at room temperature for 6 hours to facilitate the reaction. The resulting precipitate was filtered and dried under ambient conditions. The synthesized Schiff base, 1,3-bis((pyridin-2-ylmethylene)thiourea), was washed with ethanol to remove impurities and dried thoroughly. The synthesis scheme and molecular structure of the prepared Schiff base are illustrated in Figure 1.

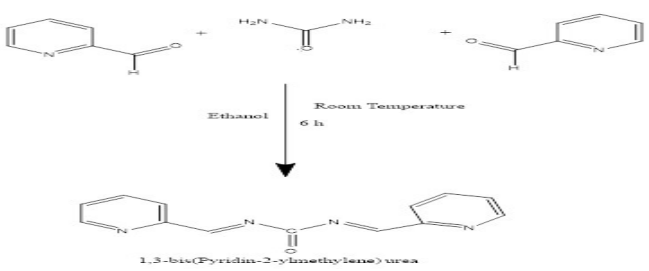

Figure.1 Synthesis of 1,3-bis(pyridin-2-ylmethylene)urea

The reaction of an aldehyde and thiourea forms a Schiff base is confirmed by the presence of vibrations representing C =N at 1656 cm-1. Observation of bands at 1522 cm-1 and 1593 cm-1 is related to the presence of the vibrations of C=C and C=N at the aromatic rings.

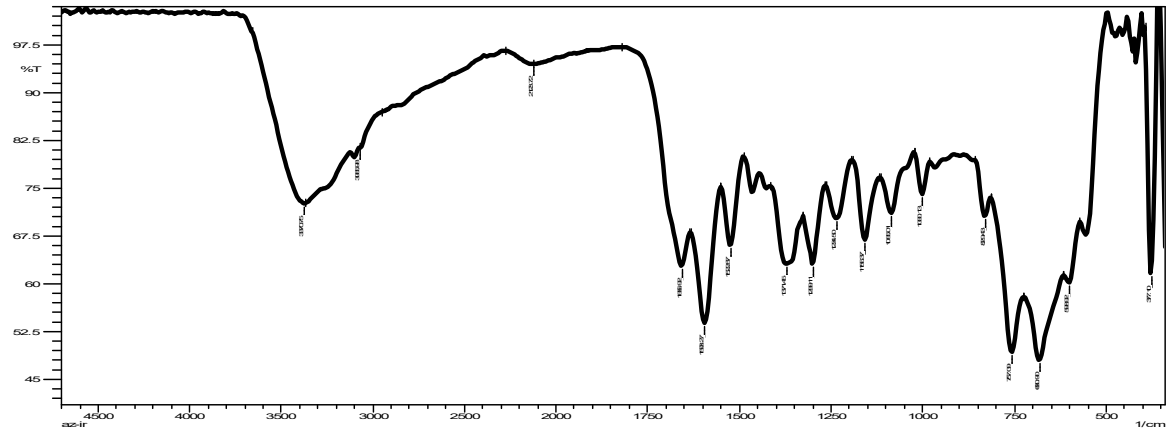

2.3 Weightloss measurements

Weight-loss measurements were carried out in accordance with the standard procedures recommended by the American Society for Testing and Materials (ASTM). Copper specimens were fully immersed for 2 hours in 100 mL of acidic solutions, both in the absence and in the presence of the inhibitor, at room temperature (301 ± 1 K). The inhibition efficiency was calculated from the average weight loss of two specimens using the following equation.

$$IE = \left(\frac{W-W'}{W}\right) X\ 100 \quad \text{(i)}$$

W and W' are the weight losses in uninhibited and inhibited solutions respectively.

2.4 Electrochemical Impedance Measurement

Electrochemical studies were performed using a conventional three-electrode system, where a saturated calomel electrode (SCE) served as the reference electrode, a platinum foil acted as the auxiliary (counter) electrode, and a Teflon-coated copper rod was used as the working electrode. After immersion of the specimen in the corrosive medium, a stabilization period of 45 minutes was allowed to ensure a stable open circuit potential (Eocp vs. SCE) before impedance measurements were initiated.

Electrochemical impedance spectroscopy (EIS) measurements were carried out at open circuit potential using a computer-controlled potentiostat (Zahner Zennium XC high-grade electrochemical instrument). Data analysis was performed using ZMAN impedance analysis software. A sinusoidal excitation signal with an amplitude of 10 mV (peak-to-peak) was applied, and the AC frequency was varied from 10 mHz to 100 kHz. The inhibition efficiency (IE%) was then determined using the following equation [30].

$$IE\% = \frac{R'_{ct}-R_{ct}}{R'_{ct}} X100 \quad \text{(ii)}$$

Where Rct and R'_{ct} are the values of charge transfer resistances in the inhibited and uninhibited solutions respectively.

2.5 Potentiodynamic Polarization measurement

Potentiodynamic polarization measurements were carried out using the same electrochemical cell configuration at a scan rate of 1.6 mV s^{-1}. The potential was swept from values more negative than the open circuit potential (OCP) to values more positive than OCP through the corrosion potential region. The inhibition efficiency was then evaluated using the corresponding relationship [30–33].

$$IE\% = \frac{i_{corr}-i'_{corr}}{i_{corr}} X\ 100 \quad \text{(iii)}$$

where the corrosion current densities of the samples with and without inhibitor are represented by the following variables i_{corr} and i'_{corr}.

2.6 Potential of Zero Charge

Electrochemical impedance spectra were obtained at various applied DC potentials using an AC signal frequency of 20 kHz. To determine the potential of zero charge (PZC), the double-layer capacitance values were plotted as a function of the applied DC potentials.

3.RESULTS AND DISCUSSION

3.1 Weightloss measurement

Table 1 shows the corrosion rate and inhibition efficiency of copper in 1.0 M HNO_3 and 0.5 M H_2SO_4 solutions at different concentrations of the inhibitor under study. The results obtained show that at increasing inhibitor concentration, the corrosion rate distinctly decreases while inhibition efficiency increases to a considerable extent in both cases. The inhibitor strongly protects the copper surface as can be seen from this trend.

Table.1 Corrosion inhibition efficiency of 1,3-bis(pyridin-2-ylmethylene)urea on corrosion of copper in higher concentration of 1.0 M HNO3 and 0.5 M acid of H2SO4.

Medium	Inhibitor Concentration (mM)	Corrosion rate (mmpy)	Inhibitor efficiency (1E%)

1.0 M HNO_3	Blank	48.02	-
	0.02	29.10	39.4
	0.05	18.00	62.5
	0.1	11.91	75.2
	0.5	7.54	84.3
	1	2.59	93.1
0.5M H_2S0_4	Blank	23.14	-
	0.02	9.42	59.3
	0.05	8.34	63.7
	0.1	5.53	76.1
	0.5	2.68	88.4
	1	1.09	94.3

The corrosion rate of copper without inhibitor in 1.0 M HNO_3 medium was 48.02 mmpy. With the addition of the inhibitor, corrosion rate decreased continuously from 29.10 mmpy at 0.02 mM concentration to 2.59 mmpy at 1 mM concentration. Inhibition efficiency rose to 94.8% simultaneously. The corrosion rate decreased significantly, which shows that the inhibitor molecules reduce metal corrosion in nitric acid medium. The inhibition efficiency determined at a concentration of 1.0 mM indicates the formation of a protective layer on the metal surface that is highly compact and adherent.

The uninhibited corrosion rate, in 0.5 M H_2SO_4 solution, was recorded as 23.14 mmpy. The corrosion rate dropped substantially with the addition of inhibitor to 9.42, 8.34, 5.53, 2.68 and 1.09 mmpy at concentrations 0.02, 0.05, 0.1, 0.5 and 1 mM respectively. The efficiency of inhibition increased with an increase in inhibitor concentration from 59.3 to 95.3. The greater inhibition efficiency exhibited in sulfuric acid medium relative to the nitric acid medium indicates stronger adsorption and more coverage of the surface with the inhibitor in H_2SO_4.

When the inhibitor concentration increases, the inhibition efficiency also increases. This is because at a certain concentration the inhibitor molecules start adsorbing on to the copper surface. With increasing inhibitor concentration, more and more active sites on the surface of metal gets occupied with inhibitor molecules, thereby improving surface coverage and formation of stable protective film [34]. The presence of the adsorbed layer acts as a barrier between the metal and the aggressive acidic medium. It reduces anodic metal dissolution as well as cathodic hydrogen evolution reactions [35].

The presence of heteroatoms and π-electrons in the molecular structure of the inhibitor may be affecting its performance by facilitating the transfer of electrons from the inhibitor to the vacant d-orbitals of copper atoms [36]. This type of interaction enhances adsorption and bolsters the stability of the protective film. Good efficiencies were observed at higher concentrations, which indicates a strong relationship between the inhibitor and copper surface. Further, the inhibitor works properly in acidic media.

The experimental results indicate that the studied inhibitor is an effective corrosion inhibitor of copper in nitric and sulphuric acid solutions. Maximum inhibition efficiencies of 94.8% were obtained in 1.0 M HNO_3 and 95.3% in 0.5 M H_2SO_4 at 1.0 mM inhibitor concentration.

3.2 Electrochemical Impedance Spectroscopy

The Nyquist impedance spectra of the copper in 1.0 M HNO_3 and 0.5 M H_2SO_4 solutions at 290 K are shown in Figures 3a and 3b, respectively, in absence and presence of different concentrations of inhibitor. The data obtained from the fitting of

the experimental data to the equivalent circuits are presented in Table 2. The Nyquist plots exhibit depressed semi-circular capacitive loops. Thus, the corrosion process is mainly controlled by charge transfer at the metal/electrolyte interface [30]. The presence of nodules in the semicircle depicts that the copper surface may not behave as an ideal capacitor. This suggests that the non-ideal behavior could be a result of the surface heterogeneity and roughness, adsorption of ionic

species, and non-uniform distribution of the active sites on the copper surface [30].

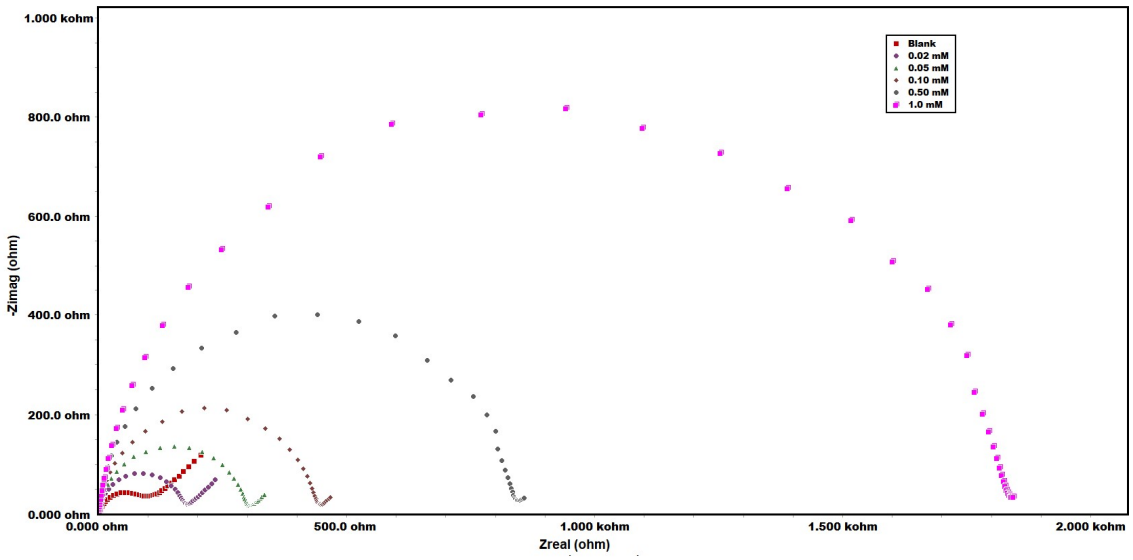

Figure.3a Electrochemical Impedance Spectra of copper corrosion in 1.0 M HNO3 in the presence and absence of Schiff base at various concentrations.

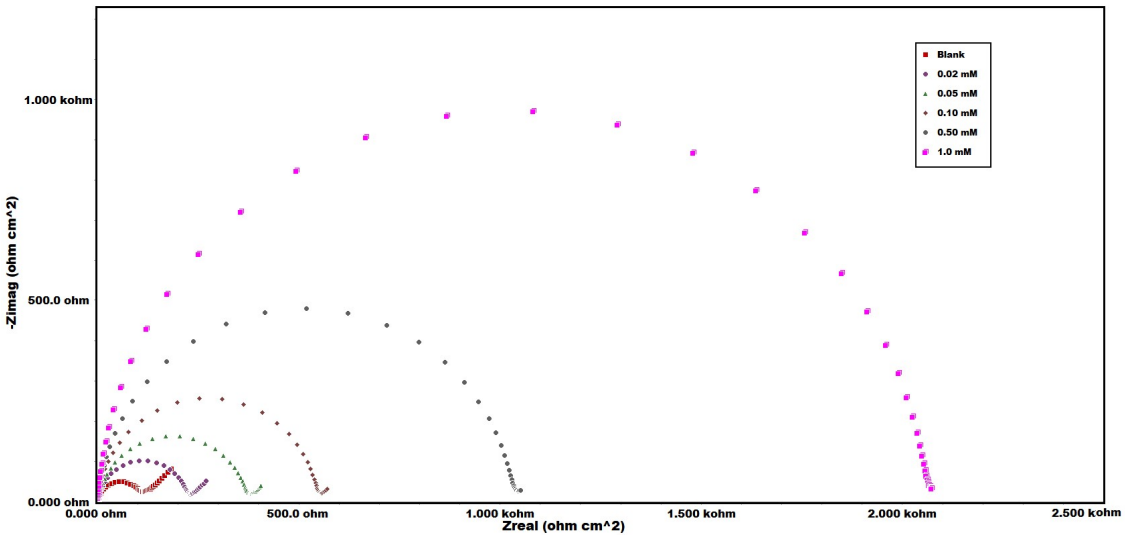

Figure.3b Electrochemical Impedance Spectra of copper corrosion in 0.5 M H_2SO_4 in the presence and absence of Schiff base at various concentrations.

With increase in inhibitor concentration in both acid media, the diameter of the capacitive semicircle was increased. The above behavior illustrates that the inhibitor effectively inhibits the corrosion reaction owing to the formation of an adsorbed film over the metal [37]. The increase in the diameter of the semicircle is correlated to higher charge transfer resistance (Rct), showing a slower rate of electron transfer from the metal to the corrosive media. The charge transfer resistance in 1.0 M HNO_3 solution was remarkably increased from 91.1 Ω cm^2 for blank solution to 1822 Ω cm^2 at 1.0 mM inhibitor concentration.

In 0.5 M H_2SO_4 medium, like the previous case, Rct values also increased from 102.7 Ω cm^2 for the uninhibited solution to 2054 Ω cm^2 at 1.0 mM inhibitor concentration with inhibition efficiency of 95 %. The notable rise in Rct readings corroborates that the inhibitor molecules are strongly adsorbed onto copper metal surface and effectively control the corrosion process.

In both the acid media, the Rs values displayed minor variations with the concentration of the inhibitors. This implies that

the inhibitor mainly modifies the interfacial electrochemical reactions and not the bulk properties of the electrolyte solution [38]. The Warburg impedance value (W) is proportional to the concentration of the inhibitor, indicating the increasing significance of diffusion-controlled processes following adsorption of inhibitor film. The inhibitor layer slows down mass transfer of corrosion-causing ions and dissolved oxygen to the metal surface, thereby diminishing the corrosion rate of the metal [39].

The constant phase element (CPE) was used in place of an ideal capacitor for better fitting of the impedance data due to the presence of depressed semicircles in the experimental Nyquist plots. According to the study, the values of “n” close to the unity of the acid solution indicate that the electrode/electrolyte interface behaves mainly as a capacitive system [30]. The slight deviation of n from unity is attributed to in homogeneities and surface irregularities of metals due to the adsorption phenomenon and roughness

[30].

The values of the admittance parameter (Y_0) and double layer capacitance (Cdl) were found to decline continuously upon increasing the inhibitor concentration in both acidic media ownward trend of Cdl value was observed by increasing the concentration of inhibitor in the acidic solution. In 1.0 M HNO_3 solution, the Cdl value decreased from 157 µF cm^{-2} for blank solution to 52 µF cm^{-2} at 1.0 mM inhibitor concentration. Similarly, in 0.5 M H_2SO_4 medium the Cdl values decreased from 224 µF cm^{-2} to 61 µF cm^{-2}. The decrease in Cdl values is due to the adsorption of the inhibitor molecules at the metal/solution interface in place of water molecules [30]. This lowers the local dielectric constant. Also, the thicker electrical double layer caused by adsorption will cause a decrease in capacitance.

Lower Y_0 values provide further evidence of the formation of a dense protective layer on copper surface. As there is more adsorption of an inhibitor molecule on the surface, blocking of active corrosion sites occurs [40]. Thus, impediments to charge transfer and enhanced corrosion protection are more pronounced. The electrochemical behavior found proves that the inhibitor acts through adsorption and provides effective protection against corrosion in nitric acid and sulphuric acid media.

The EIS obtained results show that the inhibitor possesses very good protective behavior for copper in acids. An increase in charge transfer resistance and decrease in double layer capacitance indicate the formation of a stable and adherent inhibitor film on the metal surface. The maximum inhibition efficiency of nearly 95% obtained at 1.0 mM in both acid media indicates highly effective corrosion inhibition behavior.

3.3 Potentiodynamic Polarization Studies

The potentiodynamic polarization curves of copper in 1.0 M HNO_3 and 0.5 M H_2SO_4 solutions at 290 K in the absence and presence of different concentrations of the inhibitor are presented in Figures 4a and 4b, respectively. The electrochemical parameters generated from the polarization measurements that is corrosion potential (Ecorr), corrosion current densities (Icorr), anodic Tafel slope (βa), cathodic Tafel slope (βc), inhibition efficiency (IE%) are summarized in Table 3. From the polarization curves it can be seen that addition of inhibitor significantly changes both anodic and cathodic branches which suggests that the inhibitor efficiently suppresses the electrochemical corrosion reactions taking place on the copper.

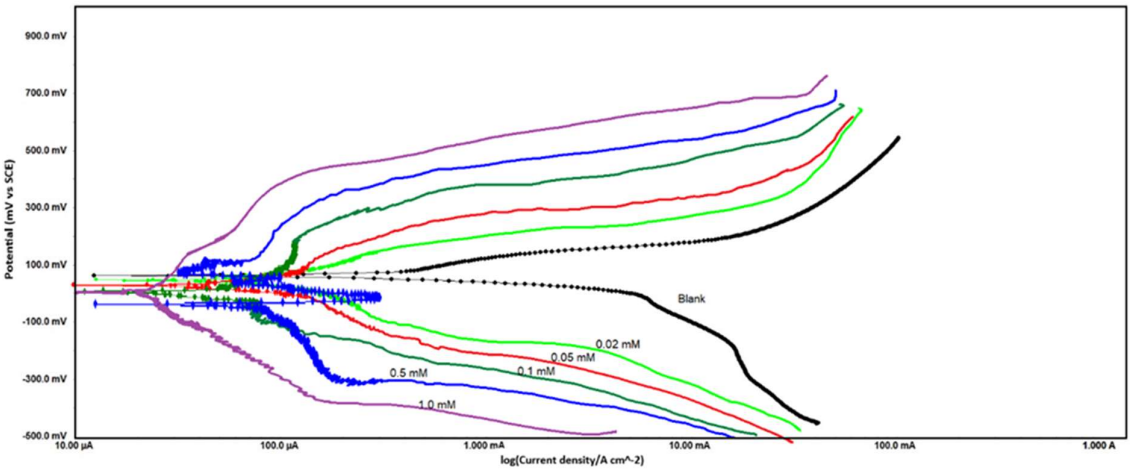

Figure.4a Tafel plots of copper corrosion in 1 M HNO_3 in presence and absence of Schiff base in various concentrations.

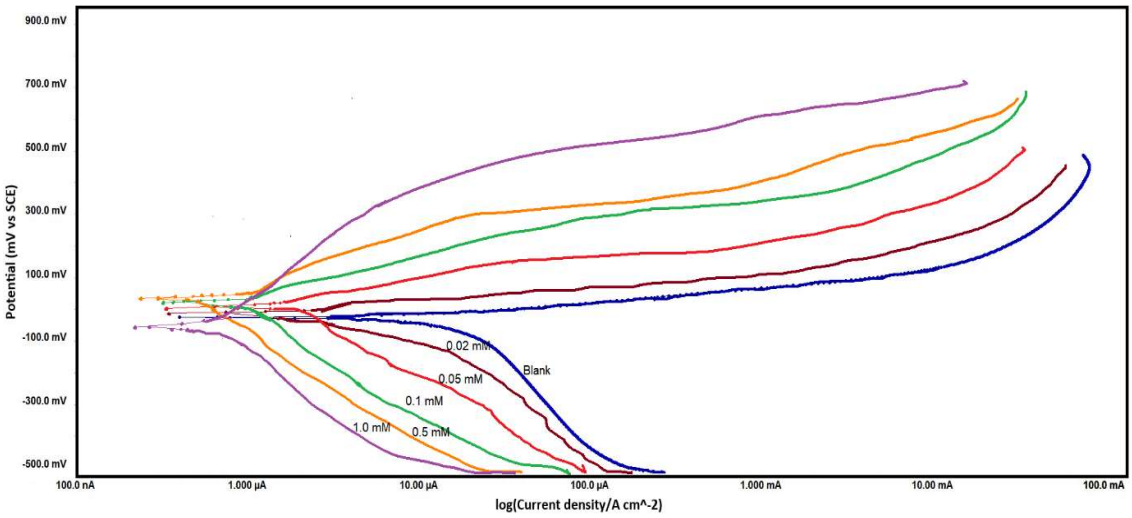

Figure.4b Tafel plots of copper corrosion in 0.5 M H_2SO_4 in presence and absence of Schiff base in various concentrations.

Corrosion current density reduced significantly in 1.0 M HNO_3 medium from a value of 388.4 µA cm^{-2} for the blank solution to 23.3 µA cm^{-2} at 1.0 mM inhibitor concentration. In accord with the increase in concentration from 0.02 mM to 1.0 mM, inhibition efficiency increased from 34%. In a similar vein, we find that in 0.5 M H_2SO_4 solution, the corrosion current density falls from 69.42 µA cm^{-2} in the uninhibited case to 2.777 µA cm^{-2} at 1.0 mM inhibitor concentration. Thus, the efficiency of inhibition here increased progressively to 96%. The inhibitor significantly slows down the rate of corrosion in both acidic environments, as evidenced by the significantly reduced corrosion current density.

Table.3 Potentiodynamic polarization parameters from corrosion of copper in 1.0 M HNO3, and 0.5 M H2SO4 acid solutions in the absence and presence of Schiff base at various concentrations.

Medium	Concentration (mM)	Ecorr (mV)	Icorr (µA cm-2)	βc (mV)	βa (mV)	IE%
	Blank	63.12	388.4	48.15	130.1	-
	0.02	56.5	256.3	112.5	92.14	34
	0.05	60.2	163.1	211.2	88.65	58
	0.1	36.5	54.38	199.4	63.32	86
	0.5	54.4	42.72	188.3	75.21	89
1.0 M HNO_3	1.0	5.02	23.3	190.7	65.31	94
	Blank	15.3	69.42	104.4	57.2	-
	0.02	20.4	29.85	147.5	60.24	57
	0.05	25.41	24.99	152.5	66.22	64
	0.1	28.38	14.58	186.4	87.35	79
	0.5	40.22	6.942	177.3	92.19	90
0.5 M H_2SO_4	1.0	3.65	2.777	183.7	62.37	96

The results showed that corrosion potential (Ecorr) values did not shift much after adding the inhibitor. The maximum shift in Ecorr values in both acid solutions did not exceed 85 mV concerning the blank solution. Based on the electrochemical criterion, an inhibitor can be said to be anodic or cathodic only when the shift in Ecorr value is more or less ±85 mV compared to the uninhibited system [30]. Given that these changes are less than this limit, the examined inhibitor may be classified as a mixed-type inhibitor. This shows that the inhibitor blocks the anodic dissolution of metal as well as the cathodic reactions both hydrogen evolution and oxygen reduction.

The anodic dissolution of the metal in acidic medium may be represented by the reaction:

$$Cu \rightarrow Cu^{2+} + 2e^{-}$$

while the cathodic reaction involving dissolved oxygen can be expressed as:

$$O_2 + 4H^{+} + 4e^{-} \rightarrow 2H_2O$$

The mechanism of anodic dissolution of the metal may be depicted by the reaction in aqueous acidic medium. The inhibitor molecules adsorb on the active sites of the metal surface and slow down the rate of both electrochemical reactions. The reduction in current densities in both anodic and cathodic directions affirm the formation of a protective adsorbed layer that

hinders the transport of electrons and hampers the influx of aggressive ions towards the metal surface. The change in Tafel slope values, both anode and cathode, was observed on increasing the concentration of inhibitor indicating that the electrode kinetics were modified after adsorption of inhibitor molecules [41].

The relatively greater variations in cathodic Tafel slopes, as compared to anodic slopes, suggest that the inhibitor influences the cathodic reaction mechanism to a greater extent. This means that the inhibitor essentially restricts the cathodic reduction reaction while still inhibiting the anodic dissolution reaction appreciably. With an increase in inhibitor concentration, a gradual decrease of corrosion current density is observed. This indicates enhanced surface coverage of the inhibitor. As more inhibitor molecules adhere to the metal surface, a tight and stable protective film develops on the surface [42]. This layer, which gets adsorbed, helps in shielding the metal from the harmful effect of acids. Further, it also prevents corrosion occurrence by reducing the active area present for acidity action.

The passive region is also absent in the polarization curves conducted using the acidic media. The absence of a well-defined passive plateau on the anodic branches suggests that the metal surface does not develop a stable oxide under the experimental conditions [43]. In strongly acidic solutions, the metal dissolves as a soluble ionic species rather than forming an oxide layer. As a result, the adsorption of inhibitor molecules is more critical than passivation for corrosion protection. To sum up, the results of Potentiodynamic polarization reveal that the tested inhibitor shows outstanding corrosion inhibition performance for copper in nitric acid and sulfuric acid. The corrosion current density is significantly decreased in the presence of inhibitor in addition to this, the inhibition efficiency values are higher and there is a slight shift in the corrosion potential that confirms the inhibitor is acting by adsorption and that it is a very good example of a mixed-type inhibitor. The maximum inhibition efficiencies of 94% and 96% in 1.0 M HNO_3 and 0.5 M H_2SO_4 respectively at 1.0 mM concentration show that the inhibitor is very effective in protection and surface coverage.

3.4 Adsorption Isotherm

Figures 5a and 5b represent the adsorption isotherm plots of the investigated Schiff base inhibitor on the copper surface in 1.0 M HNO_3 and 0.5 M H_2SO_4 solutions at room temperature. The adsorption behavior of the inhibitor molecules on the metal surface plays a significant role in the corrosion inhibition mechanism. The adsorption process can be described as a substitution reaction in which water molecules previously adsorbed on the metal surface are replaced by inhibitor molecules from the solution. This process results in the formation of a protective adsorbed film that isolates the metal from the aggressive acidic environment and suppresses corrosion reactions.

The adsorption process may be represented as [30]:

$$Org_{(sol)} + xH_2O_{(ads)} \rightarrow Org_{(ads)} + xH_2O$$

where x is the the inhibitor molecules from the solution phase replace adsorbed water molecules present on the copper surface. The extent of adsorption was evaluated using the surface coverage values (θ), which were calculated from the charge transfer resistance values obtained from impedance measurements.

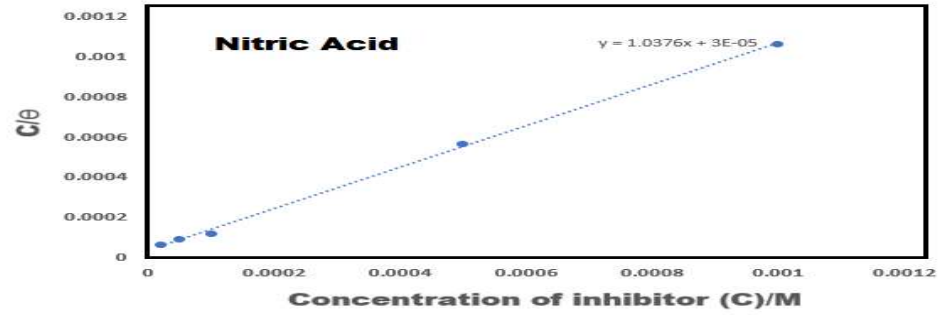

Figure.5a Isotherm of adsorption of 1, 3-bis (pyridin 2-ylmethylene)urea on copper in 1.0 M acid solution

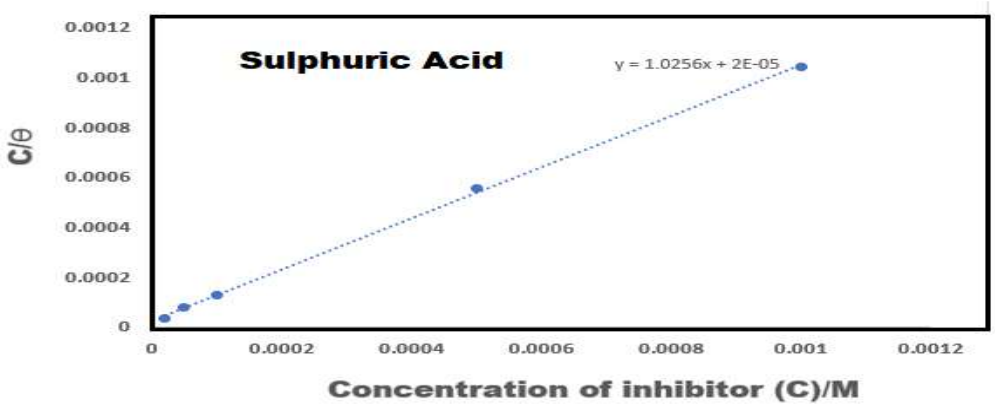

Figure.5b Isotherm of adsorption of 1, 3-bis (pyridin 2-ylmethylene) urea on copper in 0.5 M H_2SO_4 acid solution

The surface coverage was determined using the relation:

$$\theta = \frac{R'_{ct} - R_{ct}}{R_{ct}}$$

where $R_{ct}$and R'_{ct}represent the charge transfer resistance values in the absence and presence of inhibitor, respectively. An increase in surface coverage with increasing inhibitor concentration indicates progressive occupation of active corrosion sites by inhibitor molecules.

The adsorption characteristics of the inhibitor were analyzed using various adsorption isotherms, and the experimental data showed excellent agreement with the Langmuir adsorption isotherm model. The Langmuir isotherm assumes monolayer adsorption of inhibitor molecules on a homogeneous metal surface without interaction between adsorbed species. The Langmuir equation is expressed as:

$$\frac{C_{inh}}{\theta} = C_{inh} + \frac{1}{K_{ads}}$$

where $C_{inh}$is the inhibitor concentration, θis the surface coverage, and $K_{ads}$is the adsorption equilibrium constant. The linear nature of the plots of C_{inh}/θversus C_{inh}obtained for both acid media confirms that the adsorption process obeys the Langmuir adsorption model. The correlation coefficient values greater than 0.9 further support the suitability of the Langmuir isotherm for describing the adsorption behavior of the Schiff base inhibitor.

The adsorption equilibrium constant obtained from the Langmuir plots was used to evaluate the standard free energy of adsorption (ΔG_{ads}) using the following relation:

$$K_{ads} = \frac{1}{55.5}\exp\left(\frac{-\Delta G_{ads}}{RT}\right)$$

where Ris the universal gas constant, Tis the absolute temperature, and 55.5 represents the molar concentration of water in the solution. The calculated values of ΔG_{ads}were found to be −37.10 kJ mol^{-1} for 1.0 M HNO_3 solution and −34.09 kJ mol^{-1} for 0.5 M H_2SO_4 solution.

The negative values of ΔG_{ads}indicate that the adsorption of the Schiff base molecules on the copper surface occurs spontaneously in both acidic media. The relatively large negative values also suggest strong interaction between the inhibitor molecules and the metal surface. Generally, values of ΔG_{ads}less negative than −20 kJ mol^{-1} are associated with physical adsorption involving electrostatic interactions, whereas values more negative than −40 kJ mol^{-1} correspond to chemical adsorption through charge sharing or transfer between inhibitor molecules and the metal surface. The obtained values lying between −20 and −40 kJ mol^{-1} indicate that the adsorption mechanism involves both physisorption and chemisorption processes [44].

The presence of heteroatoms such as nitrogen and sulfur in the Schiff base structure enhances adsorption through lone pair electron donation to the vacant d-orbitals of iron atoms on the metal surface [45]. In addition, π-electrons present in the molecular structure may contribute to stronger adsorption interactions. Electrostatic attraction between protonated inhibitor molecules and the charged metal surface may also participate in the adsorption process in acidic medium [46].

The stronger adsorption behavior observed in nitric acid solution, as indicated by the slightly more negative ΔG_{ads}value, suggests comparatively stronger interaction of inhibitor molecules with the metal surface in HNO_3 medium. The formation of a stable adsorbed film reduces direct contact between the metal and corrosive ions, thereby minimizing charge transfer and lowering the corrosion rate [44].

Overall, the adsorption studies confirm that the Schiff base inhibitor exhibits excellent affinity toward the copper surface and protects the metal through spontaneous adsorption following the Langmuir adsorption isotherm. The combined physical and chemical adsorption mechanism contributes significantly to the high inhibition efficiencies observed in both nitric acid and sulfuric acid solutions.

3.5 Potential of Zero Charge

The variation of differential capacitance with potential for copper in 1.0 M HNO_3 and 0.5 M H_2SO_4 solutions without and with Schiff base inhibitor is illustrated in Figures 6a–6d. The results of the capacitance measurements provided important electrochemical parameters; among which we have the values of the open circuit potential (Eocp), potential of zero charge (PZC) and excess surface charge (Eocp-Epzc); these results which appear in Table 4, show that we are overcoming slight surface charge of the metal and adsorption of the inhibitor in acidic media.

The electrical charge of the metal/solution interface plays a significant role in the interaction of inhibitor molecules with metal [30,44]. The surface charge of the metal, dipole moment of the inhibitor molecules, and presence of ions like nitrate and sulphate ions which get adsorbs specifically influences the adsorption [47]. The charge characteristics of a metal surface under corrosion can be evaluated using open circuit potential values.

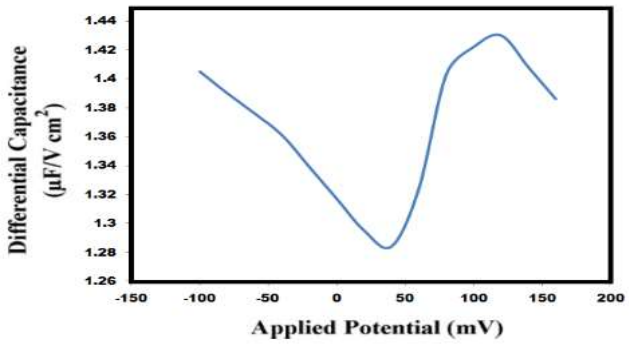

Figure.6a Differentiated capacitance vs Applied potential for copper in 1.0 M HNO_3 acid solution.

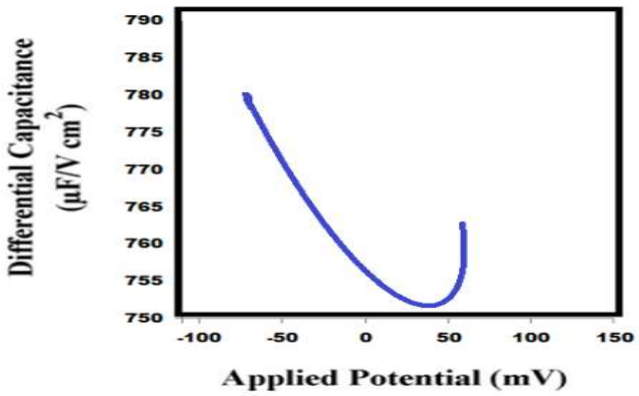

Figure.6b Differentiated capacitance verses Applied potential of copper in 1.0M HNO_3 acid solution in the presence of Schiff base.

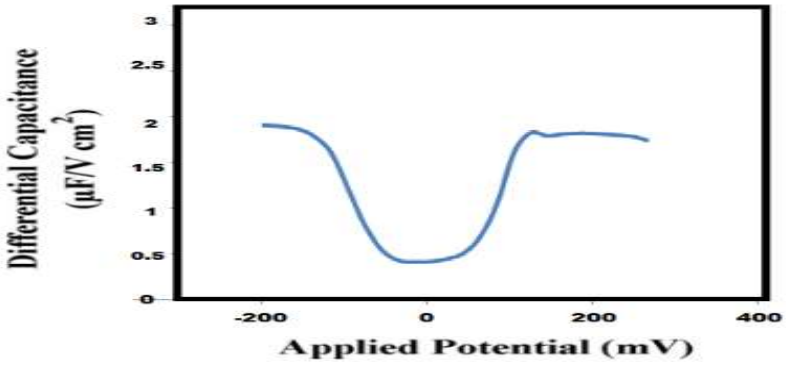

Figure.6c Differentiated capacitance vs Applied potential for copper in 0.5M H_2SO_4.

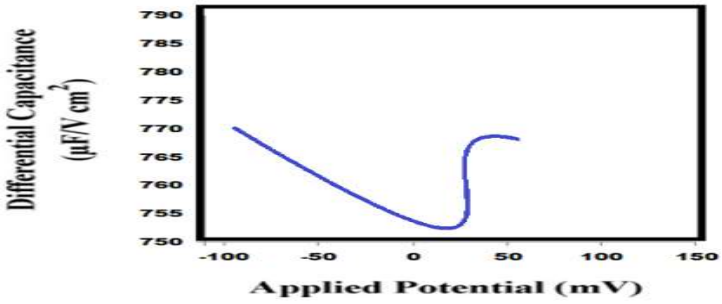

Figure.6d Differentiated capacitance vs Applied potential in copper solution in 0.5M H_2SO_4 acid in the presence of Schiff base.

The surface charge behavior was evaluated using the relation [30,44]:

$$E_r = E_{ocp} - E_{pzc}$$

where E_r represents the rational corrosion potential, $E_{ocp}$is the open circuit potential, and $E_{pzc}$is the potential of zero charge. The sign and magnitude of E_r provide information regarding whether the metal surface is positively or negatively charged in the corrosive environment.

Table.4 Overcharge on the copper metal surface of 1.0M HNO_3 and 0.5M H_2SO_4 acid solutions in the presence and absence of Schiff base.

Medium	Eocp (mV/SCE)	PZC (mV/SCE)	Excess charge Eocp- EPZC (mV)
1.0M HNO_3	+44.50	+39.5	+4.5
1.0M HNO_3 + 0.5mM of Inhibitor	+51.20	+41	+10.2
0.5M H_2SO_4	+2.60	-22	+32.60
0.5M H_2SO_4 + 0.5mM of Inhibitor	+32.60	+20	+12.60

The excess charge readings for 10 mM HCl and 10 mM Acetic acid were both positive which implies that the OCP of a copper surface is positively charged. The initial adsorption of aggressive anions such as nitrate and sulphate ions on the metal surface is believed to cause a positive surface charge. These anions that are specifically adsorbed create a conducive environment for the adsorption of protonated inhibitor species to electrostatic attraction. As a result, the inhibitor molecules are strongly attached to the pre-adsorbed anionic layer to form a stable protective layer over the metal.

The adsorption behavior of the inhibitor is supported by differential capacitance curves. When there is no inhibitor, the capacitance values are found to be relatively higher due to direct interaction of the metal with the corrosive electrolyte [48]. Upon addition of the Schiff base inhibitor, the capacitance values decrease considerably. Therefore, it can be concluded that inhibitor molecules displace water molecules and aggressive ions from the electrical double layer.

The lower than expected differential capacitance indicates the thickness of the electrical double layer is increased while the local dielectric constant at the interface is decreased due to behaviour of organic molecules [49]. The alterations seen in the capacitance–potential curves also reflect the change of the interfacial structure after inhibitor adsorption. The inhibitor affects the orientation of charged species on the metal/solution interface and decreases the size of the active surface area available for corrosion. This behavior indicates the formation of a compact adsorbed layer isolating the metal from acid.

The presence of heteroatoms like nitrogen and sulfur within the Schiff base molecule further enhances the adsorption process. These atoms have lone pair electrons which can interact with the vacant d-orbitals of iron on the metal surface. In acidic media, protonation of inhibitor molecules may also occur. This allows for an additional electrostatic interaction between the inhibitor and the adsorbed sulphate or nitrate ions. The electrostatic attraction, along with coordinate bonding, causes strong adsorption and exhibits high corrosion inhibition efficiency.

The findings of capacitance measurements and surface charge analysis show that the Schiff base inhibitor adsorbs effectively on the surface of copper in HNO3 and H2SO4 media. The formation of a stable protective adsorbed film on the surface of the metal which leads to the positive excess charge value, decrease in differential capacitance and shift in open circuit potential significantly contributes to the lowered corrosion rate of copper in acidic solutions [50].

4. Conclusion

The present investigation demonstrated that 1,3-bis(pyridin-2-ylmethylene)urea acts as an efficient corrosion inhibitor for copper in 1.0 M HNO_3 and 0.5 M H_2SO_4 acidic media. As the inhibitor concentration increased, the inhibition efficiency increased progressively which could be due to the progressive adsorption and surface coverage of the inhibitor molecules on copper surface.

The results of weight-loss measurements showed a significant corrosion rate reduction in the presence of the Schiff base, with inhibition efficiencies being approximately 95% at higher concentrations of the inhibitor. When the inhibitor was introduced in the corrosive environment, there was a notable increase in charge transfer resistance which doubled while the double layer capacitance dropped. This showed that the inhibitor had formed a protective and stable film that was firmly attached to the surface of the metal/solution interface.

Analysis of potentiodynamic polarization indicated a significant reduction in the current density of corrosion with only a minor variation in corrosion potential which shows the behaviour of the inhibitor is a mixed-type and affects both anodic and cathodic reactions.

The inhibitor isotherm follows the Langmuir model indicating the monolayer adsorption of the inhibitor on copper surface. The obtained negative values of free energy of adsorption confirm the spontaneity of adsorption and the inhibition mechanism involves the physisorption and chemisorption process.

In support of adsorption processes characterized by practically 100% efficiency in acidic solution, potential of zero charge

(PZC) curve studies showed a favorable electrostatic interaction between the protonated inhibitor molecules and copper surface. The strong inhibition efficiency of the Schiff base is due to the presence of nitrogen donor atoms and a conjugated π-electron system, which favor strong interaction with the copper surface, as well as the formation of a compact barrier film. The findings, as a whole, demonstrate that 1,3-bis(pyridin-2-ylmethylene)urea exhibits significant corrosion inhibition properties and can be seen as an effective organic inhibitor for copper protection in aggressive acidic medium.

References

1. Shinato KW, Zewde AA, Jin Y. Corrosion protection of copper and copper alloys in different corrosive medium using environmentally friendly corrosion inhibitors. Corrosion reviews. 2020 Mar 26;38(2):101-9.
2. Evans UR. Behaviour of metals in nitric acid. Transactions of the Faraday Society. 1944;40:120-30.
3. Bunce NJ, Chartrand M, Keech P. Electrochemical treatment of acidic aqueous ferrous sulfate and copper sulfate as models for acid mine drainage. Water Research. 2001 Dec 1;35(18):4410-6.
4. Samie F, Tidblad J, Kucera V, Leygraf C. Atmospheric corrosion effects of HNO3—method development and results on laboratory-exposed copper. Atmospheric Environment. 2005 Dec 1;39(38):7362-73.
5. Controlling copper corrosion in these media is essential for electrical, plumbing, and chemical process reliability. Organic inhibitors are widely used because they are effective at low concentrations and form protective films
6. Jaafar WA, Saeed RS. Synthesis, characterization and corrosion inhibition study of new heterocyclic compounds and schiff base with [Co (II), Ni (II), Cu (II) and Hg (II)] complexes. Syst. Rev. Pharm. 2020 Oct 1;11:134-43.
7. Verma C, Quraishi MA, Rhee KY. Corrosion inhibition relevance of semicarbazides: electronic structure, reactivity and coordination chemistry. Reviews in Chemical Engineering. 2023 Aug 28;39(6):1005-26.
8. Li FM, Huang L, Zaman S, Guo W, Liu H, Guo X, Xia BY. Corrosion chemistry of electrocatalysts. Advanced Materials. 2022 Dec;34(52):2200840.
9. Alam MZ, Alimuddin, Khan SA. A review on Schiff base as a versatile fluorescent chemo-sensors tool for detection of Cu2+ and Fe3+ metal ion. Journal of Fluorescence. 2023 Jul;33(4):1241-72.
10. Zhang C, Zhang Y, Shi S, Pan Y, Qin R, Zhang Y. The influence of substituent effects of polyphenols on the removal of Cr (VI): The significance of electron-donating and electron-withdrawing groups. Separation and Purification Technology. 2025 Aug 30;364:132500.
11. Kolapwar BG. Study of schiff base compounds and its derivatives. Anveshana's International Journal of Research in Pharmacy and Life Sciences. 2017;2(1):15-8.
12. Zhao S, Han F, Li J, Meng X, Huang W, Cao D, Zhang G, Sun R, Wong CP. Advancements in copper nanowires: synthesis, purification, assemblies, surface modification, and applications. Small. 2018 Jun;14(26):1800047.
13. Alsharif MA. Understanding Adsorption: Theories, Techniques, and Applications. In Adsorption-Fundamental Mechanisms and Applications 2025 Jan 28. IntechOpen.
14. Ma H, Chen S, Niu L, Zhao S, Li S, Li D. Inhibition of copper corrosion by several Schiff bases in aerated halide solutions. Journal of Applied Electrochemistry. 2002 Jan;32(1):65-72.
15. Gaber GA, Mohamed LZ, Aly HA, Hosny S. Corrosion potential and theoretical studies of fabricated Schiff base for carbidic austempered ductile iron in 1M H2SO4 solution. BMC chemistry. 2024 Sep 13;18(1):170.
16. Kuznetsov YI, Redkina GV. Thin protective coatings on metals formed by organic corrosion inhibitors in neutral media. Coatings. 2022 Jan 26;12(2):149.
17. Van de Vel E, Sampers I, Raes K. A review on influencing factors on the minimum inhibitory concentration of essential oils. Critical reviews in food science and nutrition. 2019 Feb 4;59(3):357-78.
18. Fang J, Li J. Quantum chemistry study on the relationship between molecular structure and corrosion inhibition efficiency of amides. Journal of Molecular Structure: THEOCHEM. 2002 Sep 27;593(1-3):179-85.
19. Rezaei-Sameti M, Zarei PN. NBO, AIM, HOMO–LUMO and thermodynamic investigation of the nitrate ion adsorption on the surface of pristine, Al and Ga doped BNNTs: A DFT study. Adsorption. 2018 Nov;24(8):757-67.
20. Mohery M, Mindil A, Mahran G, Alsubaie A. Eco-Friendly Copper Adsorption by a Novel Bis-Aminophosphonate: Design, Synthesis, Equilibrium, and Bioactive Applications. Water, Air, & Soil Pollution. 2025 Aug;236(8):484.
21. Messali M, Larouj M, Lgaz H, Rezki N, Al-Blewi FF, Aouad MR, Chaouiki A, Salghi R, Chung IM. A new schiff base derivative as an effective corrosion inhibitor for mild steel in acidic media: Experimental and computer simulations studies. Journal of Molecular Structure. 2018 Sep 15;1168:39-48.
22. Robinson SG, Sigman MS. Integrating electrochemical and statistical analysis tools for molecular design and mechanistic understanding. Accounts of Chemical Research. 2020 Jan 10;53(2):289-99.
23. Brusic V, Frisch MA, Eldridge BN, Novak FP, Kaufman FB, Rush BM, Frankel GS. Copper corrosion with and without inhibitors. Journal of the electrochemical society. 1991 Aug 1;138(8):2253.
24. Ikram M, Rehman S, Ali M, Schulzke C, Baker RJ, Blake AJ, Malook K, Wong H. Urease and α-chymotrypsin inhibitory activities of transition metal complexes of new Schiff base ligand: Kinetic and thermodynamic studies of the synthesized complexes using TG–DTA pyrolysis. Thermochimica acta. 2013 Jun 20;562:22-8.
25. Khan G, Basirun WJ, Kazi SN, Ahmed P, Magaji L, Ahmed SM, Khan GM, Rehman MA, Badry AB. Electrochemical investigation on the corrosion inhibition of mild steel by Quinazoline Schiff base compounds in hydrochloric acid solution. Journal of colloid and interface science. 2017 Sep 15;502:134-45.
26. Ren J, Xuan H, Dai W, Zhu Y, Ge L. Double network self-healing film based on metal chelation and Schiff-base interaction and its biological activities. Applied Surface Science. 2018 Aug 1;448:609-17.
27. Yang J, Chen Z, Zhang L, Zhang Q. Covalent organic frameworks for photocatalytic reduction of carbon dioxide: a review. ACS nano. 2024 Aug 8;18(33):21804-35.

28. Aswathi VP, Meera S, Maria CA, Nidhin M. Green synthesis of nanoparticles from biodegradable waste extracts and their applications: a critical review. Nanotechnology for Environmental Engineering. 2023 Jun;8(2):377-97.
29. Umoren SA, Solomon MM, Udosoro II, Udoh AP. Synergistic and antagonistic effects between halide ions and carboxymethyl cellulose for the corrosion inhibition of mild steel in sulphuric acid solution. Cellulose. 2010 Jun;17(3):635-48.
30. Mallaiya K, Subramaniam R, Srikandan SS, Gowri S, Rajasekaran N, Selvaraj A. Electrochemical characterization of the protective film formed by the unsymmetrical Schiff's base on the mild steel surface in acid media. Electrochimica Acta. 2011 Apr 15;56(11):3857-63.
31. Electrochemical and Surface Analysis of Salvia Officinalis Extract as a Green Corrosion Inhibitor for N80 Carbon Steel in Acidic Media. Int. J. Environ. Sci. [Internet]. 2025 Aug. 20 [cited 2025 Oct. 8];:3683-95.
32. Evaluation Of Antibacterial And Corrosion Inhibition Activities Of N,N'-Bis (Salicylidene) Ethylenediamine For Mild Steel In 1M H2SO4 . Int. J. Environ. Sci. [Internet]. 2025 Jun. 18 [cited 2025 Oct. 8];11(11s):504-15.
33. Environmentally Sustainable Corrosion Control Of Mild Steel Using A Benzene-Based Schiff Base In Hcl Solution. Int. J. Environ. Sci. [Internet]. 2025 Jul. 2 [cited 2025 Oct. 8];:1512-21.
34. Kuznetsov YI, Redkina GV. Thin protective coatings on metals formed by organic corrosion inhibitors in neutral media. Coatings. 2022 Jan 26;12(2):149.
35. Dong Z, Li B, Zhu Y. Noble-metal-free metal oxides for catalyzing acidic oxygen and hydrogen evolution reactions: recent developments and future perspectives. Energy & Fuels. 2024 Apr 11;38(14):12387-408.
36. Tan L, Li J, Zeng X. Revealing the correlation between molecular structure and corrosion inhibition characteristics of N-heterocycles in terms of substituent groups. Materials. 2023 Mar 7;16(6):2148.
37. Ma IW, Ammar S, Kumar SS, Ramesh K, Ramesh S. A concise review on corrosion inhibitors: types, mechanisms and electrochemical evaluation studies. Journal of Coatings Technology and Research. 2022 Jan;19(1):241-68.
38. Cao C. On electrochemical techniques for interface inhibitor research. corrosion science. 1996 Dec 1;38(12):2073-82.
39. Jena G, Vanithakumari SC, Polaki SR, George RP, Philip J, Amarendra G. Electrophoretically deposited graphene oxide–polymer bilayer coating on Cu-Ni alloy with enhanced corrosion resistance in simulated chloride environment. Journal of Coatings Technology and Research. 2019 Sep 15;16(5):1317-35.
40. Liu R, Zhang N, Tan B, Huang Y, Wang F, Han X, Zhao J, Zhao X. In-depth study on the influence of copper oxidation state on the adsorption of azole corrosion inhibitors: experimental, theoretical calculation, and mechanism analysis. Applied Surface Science. 2025 Sep 15;703:163427.
41. Ai JZ, Guo XP, Qu JE, Chen ZY, Zheng JS. Adsorption behavior and synergistic mechanism of a cationic inhibitor and KI on the galvanic electrode. Colloids and Surfaces A: Physicochemical and Engineering Aspects. 2006 Jun 15;281(1-3):147-55.
42. Driver R, Meakins RJ. Tafel slopes and chemical structure of inhibitors of the acid corrosion of steel. British Corrosion Journal. 1974 Jan;9(4):233-7.
43. Strehblow HH. Passivity of metals studied by surface analytical methods, a review. Electrochimica Acta. 2016 Sep 10;212:630-48.
44. Thanapackiam P, Rameshkumar S, Subramanian SS, Mallaiya K. Electrochemical evaluation of inhibition efficiency of ciprofloxacin on the corrosion of copper in acid media. Materials Chemistry and Physics. 2016 May 1;174:129-37.
45. Husaini M. Schiff Base-Derived Organic Molecules as High-Performance Corrosion Inhibitors for Metals. Journal of Applied Science and Environmental Studies. 2025;8(4):258-80.
46. Kadhim A, Betti N, Al-Bahrani HA, Al-Ghezi MK, Gaaz T, Kadhum AH, Alamiery A. A mini review on corrosion, inhibitors and mechanism types of mild steel inhibition in an acidic environment. International Journal of Corrosion and Scale Inhibition. 2021;10(3):861-84.
47. Long L, Xue Y, Hu X, Zhu Y. Study on the influence of surface potential on the nitrate adsorption capacity of metal modified biochar. Environmental Science and Pollution Research. 2019 Jan 30;26(3):3065-74.
48. Masaret GS, Al Jahdaly BA. Inhibitive and adsorption behavior of new thiazoldinone derivative as a corrosion inhibitor at mild steel/electrolyte interface: Experimental and theoretical studies. Journal of Molecular Liquids. 2021 Sep 15;338:116534.
49. Wu J. Understanding the electric double-layer structure, capacitance, and charging dynamics. Chemical Reviews. 2022 May 20;122(12):10821-59.
50. Quan Z, Chen S, Li Y, Cui X. Adsorption behaviour of Schiff base and corrosion protection of resulting films to copper substrate. Corrosion Science. 2002 Apr 1;44(4):703-15.